Experimental Investigation on the Behavior of Frames with and without Bracing under Horizontal Loading

AUTHOR(S):

WAKABAYASHI, Minoru; TSUJI, Bunzo

CITATION:

WAKABAYASHI, Minoru ...[et al]. Experimental Investigation on the Behavior of Frames with and without Bracing under Horizontal Loading. Bulletin of the Disaster Prevention Research Institute 1967, 16(2): 82-94

ISSUE DATE:

1967-01

URL:

http://hdl.handle.net/2433/124719

Bull. Disas. Prev. Res. Inst. Kyoto Univ., Vol. 16, Part 2, No. 112 Jan., 1967

Experimental Investigation on the Behavior of Frames with and without Bracing under Horizontal Loading

By Minoru WAKABAYASHI and Bunzo TSUJI

(Manuscript received October 30, 1966)

Abstract

Experiments are here conducted to determine the general behavior of steel frames under horizontal loading. Portal frames and one span two storied frames with and without bracing are tested by the application of monotonous and repeated horizontal loads. The influence of the compression bracing with a relatively large cross section on the restoring force characteristics of the whole frame, the relation between displacement amplitude and stiffness deterioration of the frame and the rate of energy absorption due to plastic deformation are discussed.

1. Introduction

In the design of multi-storied buildings, reinforced concrete or steel reinforced concrete structures are generally adopted. In these structures, shear walls as well as frames are designed so as to resist horizontal forces such as earthquake or wind forces. In recent years, much higher multi-storied buildings are being constructed with steel as the results of the less weight of the structures and excellence in its ductility. Some types of bracings are used to resist the horizontal force in the steel structures.

In the aseismic design of the structures, it is a primary object to clarify the restoring force characteristics of the structures under horizontal loading. Although some investigations into the restoring force characteristics have been made on the frames without bracing, there are found only few papers on the research of the frames with bracings[1),2)].

The load-displacement curve of steel structures is generally of the softening and monotonously increasing type when the joints are connected by welding. However, in the truss type structures and braced frames, some members sustain a large compressive force and the structures show a different type of load-displacement curve as the result of the buckling of the compression members.

The post-buckling strength of the compression members was investigated as the basic problem to determine the maximum load of a redundant truss. In many investigations an elastic perfectly-plastic axial force-displacement relationship is assumed[3),4),5)]. However, when the deflection increases under the load, the plastic zone may appear in some portion of the member and then the load may decrease in real structures.

Murray and others[7),8),9)] conducted experiments on triangular frames and warren trusses and they showed that the behavior of compression members was represented by two curves. One curve showed the elastic stability line[6)] of the member with the initial curvature and eccentricity. The other expressed

the plastic collapse line with consideration of the collapse mode. Paris and Hirano[10),11),12),13)] explained that the axial force-displacement curve of the centrally loaded column was able to express the behavior of the compression member in the elastic range, and the mechanism curve for the plastic range. They carried out buckling tests on pin-ended columns and compression tests on rigidly connected members of the trusses. The results correlated with the theory. Neal replaced the load-displacment curve in the plastic range by some straight lines[14)] and made it possible to solve the post-buckling strength of the complex structures.

From these above mentioned facts, the post-buckling strength of the compression member must be taken into account in the analysis of the braced frames. To explain the restoring force characteristics of structures, it is necessary to clarify not only the load-displacement curve in monotonous loading but also in repeated loading. The load-displacement curve of the steel structures shows generally Bauschinger's effect under the repeated loading. The curve of braced frames will indicate not only the lowering of yield load but also the deterioration of stiffness. In this report the behavior of the braced frames under monotonous and repeated loading is discussed.

Investigations on the energy absorption capacity of the structures, and of the structural members under repeated loading were conducted[15),16),17),18)]. For the aseismic design of the structures, it is desirable for the capacity to be large, since a large amound of the dissipation of energy input from the ground is expected. In this report, the result of the experiment was analyzed by equalizing the absorbed energy due to plastic deformation and the damped energy due to viscosity, and the relation between the equivalent viscous damping coefficient ratio and deflection amplitude is discussed.

2. Experimental Program

2.1. Scope of the Test

The restoring force characteristics of the braced frames are influenced by many factors such as the bracing arrangement in the frame, the type of bracing, the shape of cross section of the bracing, the stiffness ratio of the bracing to the frame.

Test specimens shown in Fig. 1 are portal frames and one span two storied frames fixed at the roots of the columns. Four kinds of portal frames are fabricated such as the SO-type without bracing, the SK-type with K-truss type bracing, the SX-type with diagonal bracing and the SZ-type with single bracing. Three kinds of two storied frames are used in the test, namely the SO-type, the SK-type and the SX-type.

The experiments are conducted for the portal frames under monotonous horizontal and also under repeated loading, and for the one span two storied frames under repeated horizontal loading.

2.2. Test Specimen

The specimen is constructed with the structural steel, SS41. For the columns and beams, rolled wide flange sections H−100×100×6×8 and H−100×50×5×7 are used respectively. The bracings are made by the welded build-up wide

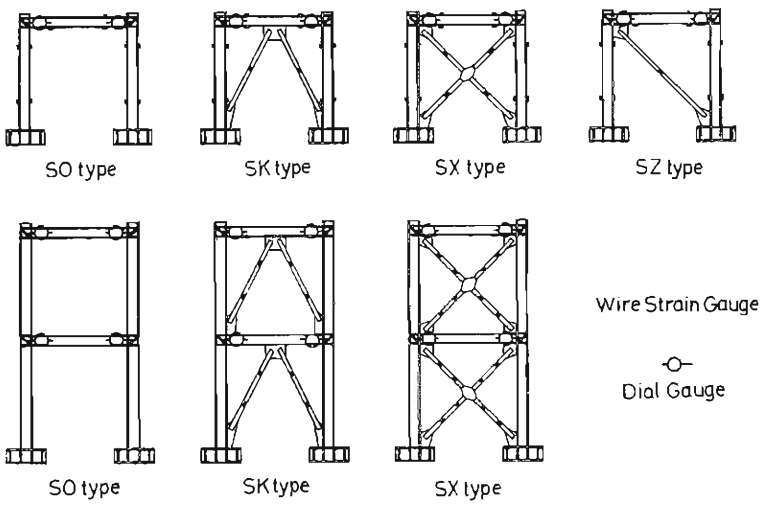

Fig. 1. Test Specimen.

flange sections H−40×30×4×4. All joints are connected by welding and at the corner of the frame a diagonal stiffner plate of 12 mm thickness is fitted to prevent the yielding in the pannel prior to the yielding of the beam and the column. For connecting the bracing to the frame, a 6 mm thick gusset plate is used. To avoid lateral buckling prior to the overall collapse in the plane of the frame, two identical frames are welded together by wide flange sections at each corner and at the mid points of the columns and beams. The principal axis of the cross sections of the bracings are arranged so as to buckle in the plane of the frame. The specimens are not annealed.

The properties of the cross-section of the specimens based on the actual measurements are shown in Table 1. The results of the tension coupon tests are indicated in Table 2 and a representative stress-strain curve is shown in Fig. 2. For the rolled wide flanges, the specimens for the coupon tests were cut out of the flange plate and for the welded flange they were cut from the original plate.

TABLE 1.
Section

		H (mm)	B (mm)	t_1 (mm)	t_2 (mm)
1 storied frame	column	100.92	100.19	6.58	7.83
	beam	101.45	49.93	4.31	6.27
	bracing	40.48	30.46	4.58	4.58
2 storied frame	column	101.02	100.23	6.14	8.04
	beam	101.44	49.49	4.17	6.34
	bracing	40.50	31.90	4.59	4.59

H ; web height t_1 ; web thickness
B ; flange width t_2 ; flange thickness

TABLE 2.
Coupon Test Results

member	thickness (mm)	width (mm)	yield stress (kg/mm²)	maximum stress (kg/mm²)	elongation (%)
column (H−100×100×6×8)	8.60	26.41	25.20	41.95	
	8.52	26.79	25.45	41.89	
	8.49	26.29	25.58	40.88	26.73
	8.42	26.55	26.18	42.02	27.66
	8.32	26.39	26.05	41.90	31.54
	8.33	26.38	25.35	41.51	25.50
	8.16	26.32	25.95	42.11	30.50
	8.32	25.87	25.10	41.00	29.10
	8.23	25.71	27.77	42.82	29.90
	8.37	25.97	26.46	42.12	29.70
beam (H−100×50×5×7)	6.44	16.01	30.75	43.12	16.88
	6.83	15.97	30.12	43.64	23.96
	6.67	15.99	31.10	43.69	23.58
	6.60	16.03	32.41	45.95	
	6.24	15.99	31.66	46.25	20.90
	6.53	15.93	32.18	44.95	23.84
	6.41	15.98	34.16	46.56	
	6.33	15.99	32.54	46.40	
	6.47	14.85	31.09	44.16	
	6.48	15.19	29.80	43.33	
	6.46	15.03	31.38	43.91	
bracing (H−40×30×4×4)	4.39	21.30	28.45	43.35	29.33
	4.34	21.53	27.50	42.91	
	4.47	21.33	29.60	47.25	
	4.39	21.51	27.55	45.56	21.20
	4.39	21.50	28.58	45.41	23.40
	4.58	21.52	28.73	44.78	

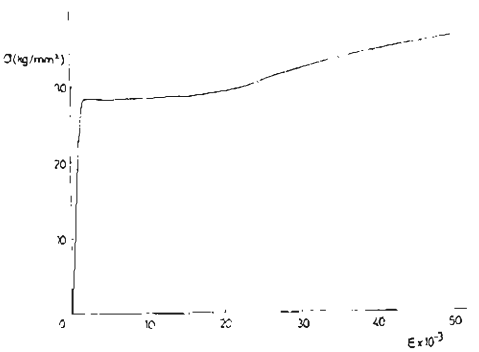

Fig. 2. Stress-Strain Curve.

2.3. *Experimental Equipment and Method*

An outline of the loading epuipment is shown in Fig. 3. The specimen is rigidly connected to the loading frame at the roots of the columns by high-tensile bolts and they form a beam. Supporting the beam at both ends, a concentrated load is applied at the column base by a hydraulic testing machine. Horizontal load acting at the top of the sup-

port is measured as the reaction of the support by a load cell. The loading frame is made rigid enough not to distort under the load. When the load is applied the specimen distorts, and the direction of the loading deviates from the initial one due to the asymmetry of the beam and loading. But as far as the infinitesimal deformation is concerned the behavior of the specimen is not influenced by the deviation.

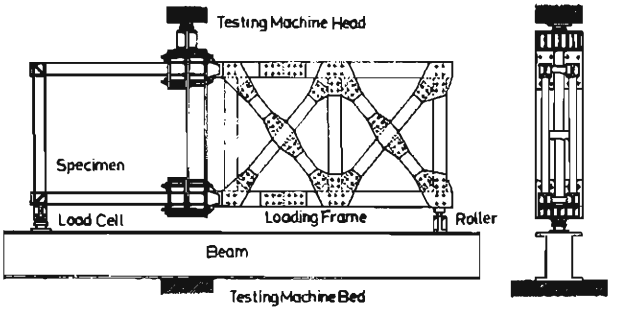

Fig. 3. Experimental Equipment.

As shown in Fig. 1, horizontal displacements are measured by dial gauges at all corners of the frame at each story, and stress distribution is measured by wire strain gauges. Rotational angles at each column base due to the distortion of the high-tensile strength bolts and elongation of the tensile bracing are measured by dial gauges as shown in Photos 1 and 2.

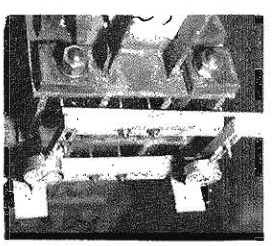

Photo. 1.

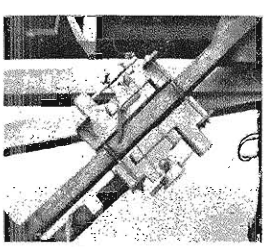

Photo. 2.

In the statical test, load is applied until local failure or lateral buckling is observed at some portion of the frame. Repeated loading is applied by increasing the deflection amplitude at each half cycle, and the loading direction is reversed at the end of each half cycle by turning the beam upside down.

3. Experimental Results

3.1. Behavior and Collapse Mode

The behavior of the specimen is analysed with attention being paid to the local or lateral buckling of the frame and to the buckling and post-buckling behavior of the compressive bracing.

Table 3 shows the relation between the horizontal displacement of the frame at the instant of the buckling of the compression bracing and the length of the

bracing. The longer the length of the bracing, the smaller is the displacement when the buckling occurs. In the case of repeated loading, the displacement at the instant of buckling from the original point of the loading becomes smaller with the increase of the displacement amplitude. But the displacement from the maximum point in one half of the prior loading cycle indicates a nearly constant value. Structures composed of elements having a different stiffness and strength produce large residual stresses under repeated loading. In the experiment, compressive residual stress arises in the compression bracing. This compressive residual stress causes the buckling at a smaller displacement from the original point in each half loading cycle. An exception is observed in the frame with K-truss type bracing. In this case, the joint of the frame and bracing displaces vertically as well as horizontally.

Table 3 also shows the relation between the axial force of the beam and the displacement when the local or lateral buckling of the beam occurs. In the case of large axial force, small displacement is observed when the buckling

TABLE 3.

specimen	axial force of beam	δh_1 (mm)
S O 1m	N	32.00
S O 1a	N	25.52
S K 1m		23.29
S K 1a		20.50
S X 1m	N+T	26.89
S X 1a	N+T	22.71
S Z 1m	N+T	41.48
S Z 1m	N	31.04
S Z 1a	N or N+T	30.51

specimen	δh_2 (mm)					length of bracing (cm)
	1st. cycle	2nd. cycle	3rd. cycle	4th. cycle	5th. cycle	
S K 1m	2.41					111.8
S K 1a	2.79	2.38	3.43	3.52	2.82	
		(4.87)	(7.13)	(8.43)	(9.92)	
S X 1m	4.49					70.7
S X 1a	3.15	3.97	3.91	1.82		
		(6.55)	(6.81)	(5.81)		
S Z 1m	2.33					141.4
S Z 1a	2.38	2.38	1.18			
		(5.98)	(5.77)			

δh_1 : horizontal displacement at the instant of local buckling
δh_2 : horizontal displacement at the instant of buckling of compression bracing
m : monotonous loading
a : alternative loading
( ) : displacement from the maximum point in one half of the prior loading cycle

occurs. In the repeated loading condition, local buckling occurs at 10 to 20% smaller displacement than with monotonous loading. Buckling in the frame with the K-truss type bracing occurs at a relatively smaller displacement than the frames of the other types. In this frame the buckling occurs at the middle point of the beam due to the vertical force from the bracing.

Some specimens tested are shown in Photos 3 to 6. The tension bracings have yielded under uniform tension, while the compression bracings have collapsed with the yield hinges at the middle and end sections. Yield hinges are also observed at each end section of the beams and the column bases of the frame. An exception is recognized in the SK-type specimen, in which a yield hinge forms at the mid point of the beam due to the vertical force. In this case tension bracing is not particularly elongated.

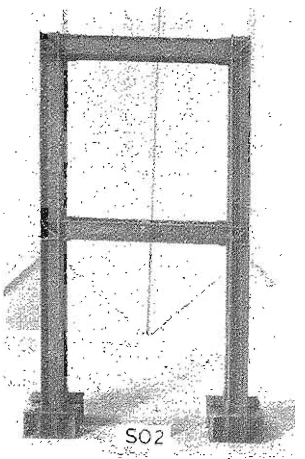

Photo. 3.

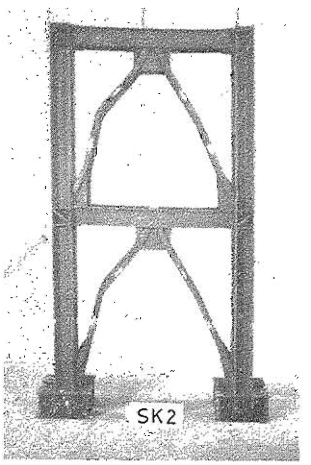

Photo. 4.

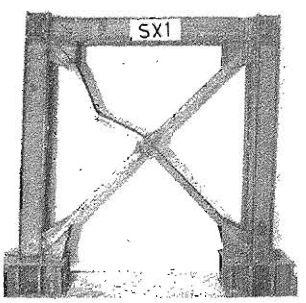

Photo. 5.

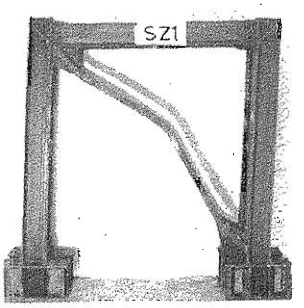

Photo. 6.

3.2. Load-Displacement Curve

Horizontal load-displacement curves at the top of the column for each specimen are shown from Figs. 4 to 10. The dotted line and the solid line show the results for the monotonous and repeated loadings, respectively.

For the frames without bracing the curve shows the softening type, and with the increase of displacement the load increases. Under repeated loadings, the

curve is of the spindle-shape, and the slope of the curve in the process of unloading is nearly equal to the initial one even after being subjected to large deflection. But with the increase of deflection amplitude the yield load decreases gradually.

The frames with bracing show a different behavior under the repeated loadings from under the monotonous one. The strength of the frames subjected to the monotonous loading is little larger than the repeated one, and the load-displacement curve at the repeated loading approaches asymptotically to that at the monotonous loading. Under the monotonous loading, the curve for the frame with the single tension bracing shows the same type as that of the frame without bracing. But the frames with compression bracing show an unstable equilibrium after the buckling of the compression bracing, and with the increase of deflection the load increases a little or keeps a nearly constant value. Under repeated loading, the curve is the same as that of the monotonous loading in the range of small deflection amplitude. With the increase of the deflection amplitude an unstable equilibrium disappears and the curve shows a spindle-shape. In this case the slope of the curve at unloading deteriorates from the initial one, and the yield load decreases gradually with the increase of deflection amplitude.

The braced frames show very complicated hysteresis loops under the repeated loadings as the result of the residual stress and the buckling deformation. It is difficult to calculate the whole loop theoretically, so under simplified assumptions the general behavior is analysed.

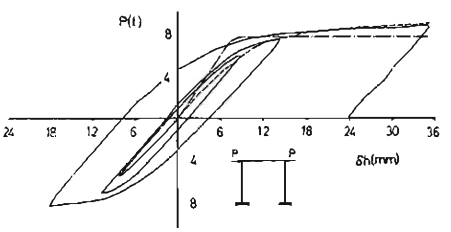

Fig. 4. Load-Displacement Curve (SO 1).

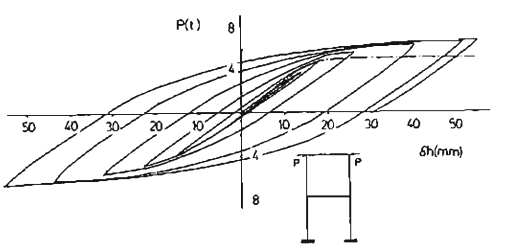

Fig. 5. Load-Displacement Curve (SO 2).

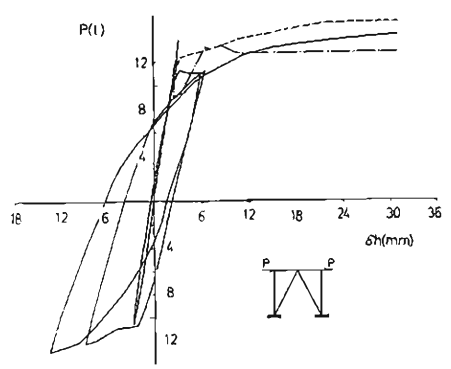

Fig. 6. Load-Displacement Curve (SK 1).

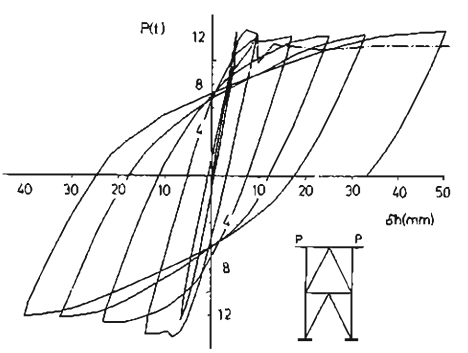

Fig. 7. Load-Displacement Curve (SK 2).

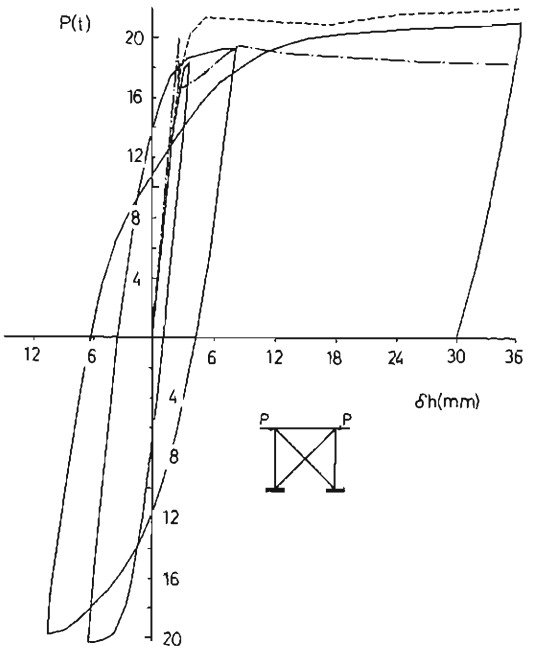

Fig. 8 Load-Displacement Curve (SX 1).

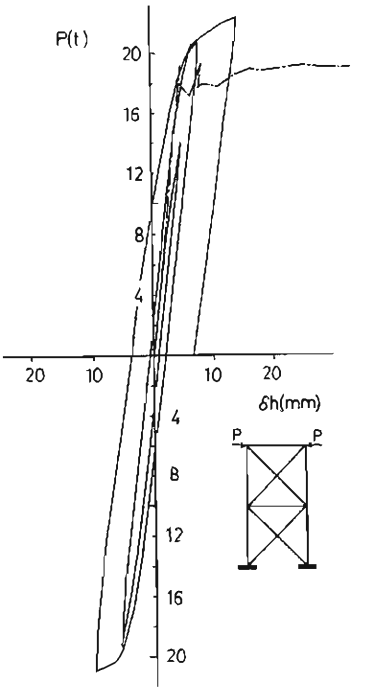

Fig. 9. Load-Displacement Curve (SX 2).

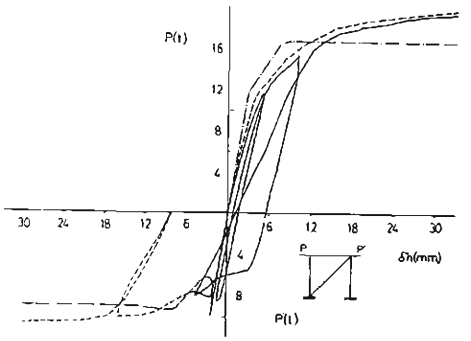

Fig. 10. Load-Displacement Curve (SZ 1).

In the load-displacement curves of the frames tested, the calculated curves under monotonous loading are indicated by dot-and-dash lines. The method of theoretical calculation is explained in Appendix 1. In the elastic range the experimental values coincide fairly well with the theoretical ones. At the instant of the buckling of the compression bracing, the experimental curve does not show such a sharp point as seen in the calculated one, due to the secondary moment. In the inelastic range, the experimental value is a little larger than the calculated one, due to the strain-hardening effect of the material and the shortening in the effective length of the members by fitting the gusset plate.

It is also observed from the load-displacement curves that the initial slope of the curve hardly deteriorates in the case of the frames without bracing, but in the case of the frames with bracing it deteriorates with the increase of the deflection amplitude. This is caused by the deterioration in the tensile stiffness of the bracing due to the buckling deformation. The amount of deterioration

at the zero load point is estimated by the method outlined in Appendix 2, assuming that the behavior of the frame is elastic in the process of unloading.

Fig. 11 shows the relation between the amcunt of stiffness deterioration and the deflection amplitude. The stiffness of the frame without bracing scarecely deteriorates even at the large deflection amplitude. At the small deflection amplitude, the experimental and calculated values of the stiffness coincide well, but under a large deflection the experimental value becomes smaller. This is due to the fact that initial curvature is found on the compression bracing as shown in Photo 4, and that the large amount of residual stress should exist in the case of repeated loading.

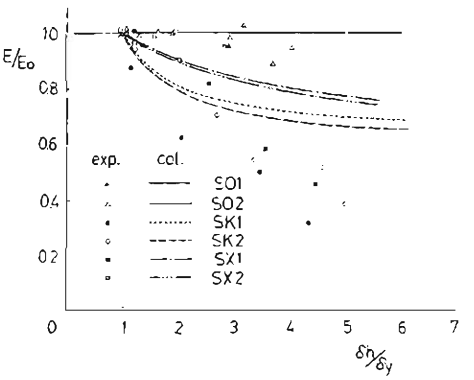

Fig. 11. Stiffness Deterioration Curve.

3.3. *Equivalent Viscous Damping Coefficient Ratio*

Steel structure can absorb a large amount of energy during the process of plastic deformation. The capacity of energy absorption should be large from the view point of the aseismic design of the structures. The relation between the equivalent viscous damping coefficient ratio ν_{eq} and deflection amplitude is deduced from the load-displacement curves which are obtained from the experiments and these relations are represented in Fig. 12. In this analysis energy absorbed by the plastic deformation is assumed to be equal to the damped energy in the linear system of one degree of freedom when it has viscous damping. In the case of the frames without bracing, the value of ν_{eq} grows large with the increase of the deflection amplitude. The frames with bracing have a large value of ν_{eq} even under a small deflection amplitude, but the value does not increase in the same proportion. SK-type frames show a nearly constant value of ν_{eq} even at large displacements, because the stiffness deteriorates considerably. SX-type frames show larger value in ν_{eq} than SK-type frames.

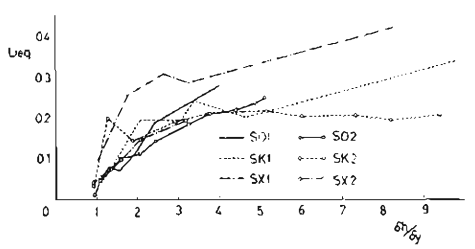

Fig. 12. Equivalent Viscous Damping Coefficient Ratio.

4. Concluding Remarks

From the experiments conducted on the portal frames and one span two-storied frames with and without bracings, the following important information is obtained.

1. The frames without bracing show the load-displacement curves of a softening type and the curves of a spindle-shape under the repeated loadings.

2. The frames with bracing show an unstable equilibrium after the buckling of the compression bracing. Under repeated loadings the load-displacement curve is the same as that of the monotonous loading in the range of small deflection amplitude. With the increase of the deflection amplitude, the curve shows a spindle-shape and the slope of the curve in the process of unloading deteriorates from the initial one.
3. When the beam is subjected to a large axial force, a small displacement is observed at which the local buckling occurs. Under repeated loadings local buckling occurs at 10 to 20% smaller displacement than that under monotonous loading.
4. The bracings connected rigidly to the frame collapse forming yield hinges at the end and middle sections under compressive force.
5. In the case of the frames with K-truss type bracing, the vertical force is induced at the middle point of the beam after the buckling of the compression bracing. The rigidity and the strength of the beam must be large enough to fully utilize the strength of the tension bracing.
6. The equivalent viscous damping coefficient ratio which indicates the capacity of the energy absorption due to the plastic work becomes large with the increase of the displacement amplitude in the case of the frames without bracing. The frames with bracing show a large value in the ratio at small deflections and with the increase of the deflection show slightly larger or nearly constant values. The ratio of SX-type frames is larger than SK-type frames.

Appendix 1. Load-Displacement Curve.

The dot-and-dash line in the load-displacement curves is calculated by a method whose underlying assumptions are stated in the following.
1. The material is considered to be distributed along the lines through the center of gravity of the section.
2. The bending moment-curvature relationship is idealized by two straight lines, one of which starts from the origin while the other is parallel to the abscissa and shows a constant.
3. Deflection due to the shearing stress is disregarded.
4. For the tension bracing, the axial force-displacement relation shows elastic perfectly-plastic behavior.
5. The compression bracing collapses forming yield hinges at the end and middle sections after its buckling.

The detailed method calculating the axial force-displacement relationship of the compression bracing is indicated in the following.

The bracing is centrally loaded, and the buckling load N_{cr} is calculated by the Euler load or tangent modulus theory

$$N_{cr}=\frac{4\pi^2EI}{l^2}\text{ or }\frac{4\pi^2E_tI}{l^2} \qquad \cdots\cdots\cdots(1)$$

where l is the length of the member, E Young's modulus, E_t the tangent modulus and I the moment of inertia.

The deflection proceeds at the buckling load until the bending moments M_m at the end and middle sections reach the fully plastic moment M_{PN}. The deflection curve after the buckling is assumed as follows,

$$y=y_m \cos\frac{2\pi x}{l} \qquad \cdots\cdots(2)$$

where x denotes the coordinate along the member. The total axial displacement Δl is composed of the shortening Δl_1 due to the axial force and the displacement Δl_2 due to the increase of the deflection, i.e.

$$\Delta l=\Delta l_1+\Delta l_2=\frac{N}{EA}l+\frac{1}{2}\int_0^l y'^2dx=\frac{N}{EA}l+\frac{\pi^2 y_m^2}{l} \qquad \cdots\cdots(3)$$

After the bending moments at the end and middle sections reach the fully plastic moment, the moment equilibrium is expressed as

$$M_m=Ny_m \qquad \cdots\cdots(4)$$

where M_m benotes the bending moment at these points and N is the axial force.

The interaction for the wide flange section subjected to the axial force and and bending moment about its weak axis is regarded as similar to that for the rectangular cross sections, that is

$$\frac{M_m}{M_p}+\left(\frac{N}{N_y}\right)^2=1 \qquad \cdots\cdots(5)$$

where M_p and N_y denote the fully plastic moment and yield axial force.

After the bending moment attains the plastic moment at the end and middle sections, the deflection is produced only by rotations at these points. The relation between the axial force and displacement is

$$\Delta l=\frac{N}{EA}l+\frac{\pi^2 y_{mp}^2}{l}+\frac{8}{l}(y_m^2-y_{mp}^2) \qquad \cdots\cdots(6)$$

where y_{mp} denotes the deflection at which the bending moment reaches the fully plastic moment. For the pin-ended bracing the axial force displacement relation can be calculated in the same manner. In Figs. 13 and 14, the calculated axial force-displacement curves are shown for the cases of the bracing rigidly jointed to the frame and for the hinged one, respectively. The dotted line is calculated on the basis of the assumption as presented by Paris that the deflection curve in the plastic range is the same as that in the elastic range.

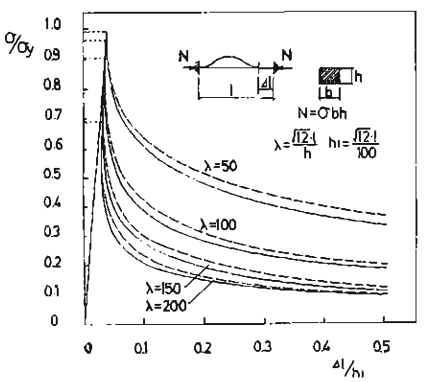

Fig. 13 Axial Force-Displacement Curve

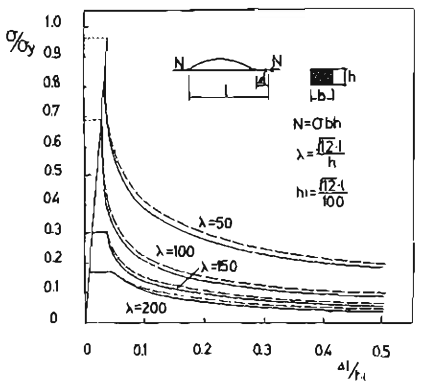

Fig. 14 Axial Force-Displacement Curve

Appendix 2. Deterioration of Stiffness.

The theoretical curves in Fig. 11 are obtained in the following manner.

1. The residual deflection of the bracing due to the buckling is of a cosine curve, that is,

$$y=y_m \cos\frac{2\pi x}{l} \qquad \cdots\cdots(7)$$

2. The bracing sustaining tensile forces at the previous loading cycle has no initial deflection for the next cycle.

3. Joints displace only in the horizonal direction.

When the axial force ΔN is imposed, the bending moment ΔM_m and the change of the deflection Δy_m at the end and middle sections are

$$\Delta M_m=\Delta N(y_m-\Delta y_m)=EI\Delta y_m\left(\frac{2\pi}{l}\right)^2 \qquad \cdots\cdots(8)$$

$$\Delta y=\Delta y_m \cos\frac{2\pi x}{l} \qquad \cdots\cdots(9)$$

The axial displacement due to the change of the deflection is

$$\Delta l_2=\frac{1}{2}\int_0^l(\Delta y)'^2 ds=\frac{2\pi^2 y_m \Delta y_m}{l} \qquad \cdots\cdots(10)$$

where ds is the length element along the member. Then the tensile stiffness D of the member with the residual deflection is expressed in the following form, taking into account the axial elongation of the member,

$$D=\frac{D_1 D_2}{D_1+D_2} \qquad \cdots\cdots(11)$$

where

$$D_1=\frac{EA}{l}, \qquad D_2=\frac{2EI}{l{y_m}^2} \qquad \cdots\cdots(12)$$

and A denotes the sectional area of the member.

References

1) N. Onitake, "An Experimental Study on Frames with Double Bracing of Light Gauge Steel," Trans. of A. I. J., No. 89, 1963. (in Japanese)
2) K. Mizuhata, "Elasto-Plastic Analysis of Framed structures with Diagonal Bracing," Disaster Prevention Research Institute Annuals, No. 7, 1964. (in Japanese)
3. R. Tanabashi, "Calculation of the Safe Maximum Load on Indeterminate Trussed Frames," Trans. of A. I. J., No. 18, 1940. (in Japanese)
4. R. Tanabashi, "On the Mechanism of Indeterminate Structures Composed of Members Deforming Non-Linearity," Trans. of A. I. J., No. 22, 1941. (in Japanese)
5) E. F. Masur, "Post-Buckling Strenght of Redundant Trusses," Proc. A. S. C. E., Vol. 79, No. 332, 1953.
6) W. Merchant, "The Failure Load of Rigid Jointed Frameworks as Influenced by Stability," Structral Engr., July, 1954.
7) N. W. Murray. "The Determination of the Collapse Loads of Ligidly Jointed Frameworks with Members in Which the Axial Forces are Large," Proc. I. C. E. Vol. 5, No. 1, 1965.

8) N. W. Murray, "Further Tests on Braced Frameworks," Proc. I. C. E., Vol. 10, 1958.
9) J. G. Nutt, "The Collapse of Triangulated Trusses by Buckling within the Plane of the Truss," Structural Engr., May, 1959.
10) M. Hirano, "Ultimate Loads of Trussed Beams—— 'Compression type' Plastic Hinge," Trans. of A. I. J., No. 66, 1960. (in Japanese)
11) M. Hirano, "Ultimate Loads of Trussed Beams——Tests on 'Compression Type' Plastic Hinge," Trans. of A. I. J., No. 69, 1961. (in Japanese)
12) M. Hirano, "Loading Capacity of Continuous Trussed Beams——Model Tests," Trans. of A. I. J., No. 96, 1964. (tn Japanese)
13) P. C. Paris, "Limit Design of Columns," Jour. of Aero. Sci., Vol. 21, No. 1, 1954.
14) B. G. Neal and D. M. Griffiths, "The Collapse of Rigidly-Jointed Singly Redundant Light Alloy Trusses," Structural Engr., December, 1963.
15) G. S. von Heydekampf, "Damping Capacity of Materials," Proc. of A. S. T. M., Vol. 31, 1931.
16) R. Tanabashi, "Test to Determine the Behavior of Welded Joints of Structural Steel under Alternate Bending Moment," Jour. of J. W. S., Vol. 7, 1939. (in Japanese)
17) L. S. Jacobsen, "Damping in Composite Sturctures," Proc. of 2nd. W. C. E. E., 1960.
18) K. Kaneta, "Study of Structural Damping and Stiffness in Nailed Joints," Disaster Prevention Research Institute Annuals, No. 3, December, 1965. (in Japanese)
19) M. Wakabayashi, "The Restoring Force Characteristics of Multi-Story Frames," Bulletin of the Disaster Prevention Research Institute, Vol. 14, February, 1965.
20) M. Wakabayashi and B. Tsuji, "Experimental Studies on the Elasto-Plastic Behavior of Steel Portal Flames with Wide Flange Section Under Repeated Horizontal Loading," Disaster Prevention Research Institute Annuals, No. 9, March, 1966.